

Research Article

IMPURITY PRODUCTION IN TOKAMAK AND THEIR RADIAL PROFILES

Jadhav A.N

Department of Electronics, Yeshwant Mahavidyalaya, Nanded Affiliated to Swami Ramanand Teerth Marathwada University, Nanded

ARTICLE INFO

Article History:

Received 06th May, 2015
Received in revised form 14th June, 2016
Accepted 23rd July, 2016
Published online 28th August, 2016

Key Words:

Electron temperature, Electron density, Ion temperature, Ion density, Radial profile, Tokamak.

ABSTRACT

The plasma parameters like the electron temperature, electron density, ion temperature, ion density etc do not have uniform values across the plasma column in the tokamak. The properties of tokamak plasma column may be studied in detailed by investigating the spatial distribution of the parametric values of the plasmas. The electron temperature and density are assumed to have the profiles like zero order Bessel function. With this assumption the radial profiles of fractional densities of the ions and spectral emission are obtained and are studied. The radial profiles of the fractional abundance of ions are obtained for different electron temperature on the axis and are presented graphically. The profile show well shaped structure. Except neutral species, fully ionized species and all the ions show similar behavior. From the study of the intensity distribution, the temperature profile may be obtained. The radial profiles of ions are useful for knowing the fractional abundances of an impurity ion at a particular distance from the axis of the plasma column. The three dimensional presentation of impurity ions at particular axial electron temperature indicates spatial distribution of ions of interest.

The radial profiles obtained for tokamak plasma show good agreement with the experimentally observed results. It may be considered that the study of radiation of impurities helps in the determination of electron temperature.

Copyright © Jadhav A.N., 2016, this is an open-access article distributed under the terms of the Creative Commons Attribution License, which permits unrestricted use, distribution and reproduction in any medium, provided the original work is properly cited.

INTRODUCTION

Tokamak

Tokamak is promoted by L.A.Artzimovich in the U.S.S.R. A tokamak is an axisymmetrical toroidal system (present systems have a major radius $R_0=100- 300$ cm) in which a hot and rather dense hydrogen or deuterium plasma is confined within a poloidal magnetic field B_p created by the current I_p flowing through it (typical values are $I_p= 100$ to 1000 kA and $B_p = 1$ to 5 kG). The plasma column remains stable against magnetohydrodynamic motions provided a strong toroidal magnetic field B_t ($B_t = 10 - 100$ kG, depending on the type of tokamak and operating conditions exists within the plasma. The magnetic-field lines formed by the superposition of poloidal and toroidal fields are helices which revolve around a toroidal axis on surfaces called magnetic surfaces (figure 1), confining the plasma ions and electrons by forcing them to move along helical orbits around the field lines [1].

The confining field is characterised by its strength and the safety factor Q (which is, physically, the number of revolutions around the torus axis after which a field line closes on itself), depending on r , B_t , I_p and R_t . It is this torsional property of the

field lines around the torus which gives the tokamak its equilibrium and stability characteristics.

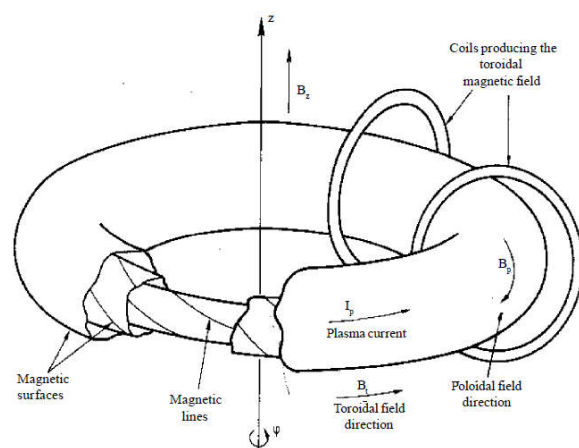


Figure 1 Magnetic configuration in Tokamak

The toroidal field B_t is produced by external coils surrounding the plasma column, whereas the plasma current is produced by inductive coupling with coils which have the same axis as the torus. The transient plasma current usually has a quasi-steady-state flat top lasting from 0.1 sec to several seconds. Note that,

*Corresponding author: **Jadhav A.N**

Department of Electronics, Yeshwant Mahavidyalaya, Nanded Affiliated to Swami Ramanand Teerth Marathwada University, Nanded

besides its stability property, I_p also heats the plasma via resistive ('ohmic') heating. A third field B_v in the vertical direction is needed to counteract the natural tendency for a current ring to expand. That is poloidal magnetic pressure $B_p^2/8\pi$ being larger on the inside, tends to increase the major radius of the plasma. The field B_v is directed so that the $J \times B_v$ force is radially inward. This field can be produced by external coils or by the image current in a highly conductive copper shell. The current channel is limited by a limiter tangential to the magnetic surface with minor radius $r = a$ (typical values of $a = 10 - 80$ cm). The most used materials are molybdenum, stainless steel (or similar alloys) and graphite; formerly tungsten was also used.

Impurity Production in Tokamak

Besides the basic gas ions (generally protons and deuterons), tokamak plasmas always contain traces of impurity ions, produced by interaction with limiter and /or the liner, such interactive ions are generally referred to as plasma wall interaction phenomena [2].

The observed impurity elements (elements as heavy as tungsten and gold have been detected) can be broadly divided into two classes, according to the mechanism responsible for their production at the walls and / or the limiter, i.e. desorbed and eroded impurities. Light impurities like Nitrogen, Oxygen and Chlorine, which are completely stripped in the centre of tokamak discharges and which therefore do not emit central line radiation are called as desorbed impurities and heavy impurities like Ti, Fe, Cr and Ni which can only be partly stripped in these plasmas since the ionisation potential χ_z of their last hydrogen like ion is much higher than the central electron temperature and are called as eroded impurities.

The principal processes by which the wall material can be removed are sputtering, unipolar arcs and evaporation. Sputtering occurs due to plasma ions, charge exchange neutrals and possibly impurity ions.

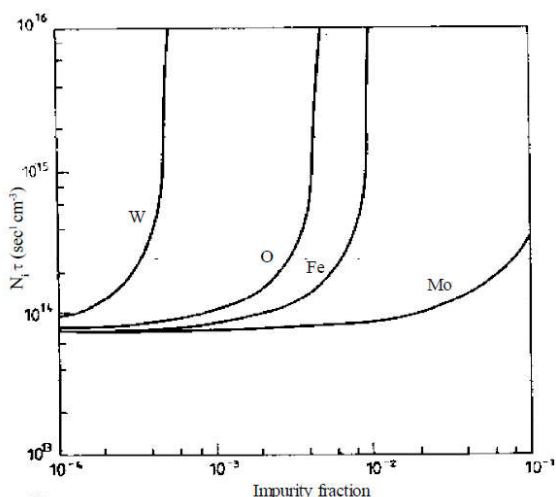


Figure 2 requirements as a function of impurity fraction for break-even experiments at 10 keV.

An impurity atom is ionized by electron impact to successively higher charge states as it penetrates progressively into the discharge where it finds an increasing electron temperature. The radial velocity of this movement perpendicular to the field lines is much smaller (typically 10^3 cm/sec) than the thermal

velocity of the unimpeded movement along the magnetic field lines (having typical values greater than 10^5 cm/sec), which leads rapidly to a uniform spread over the magnetic surfaces. Because of this reason the impurity ion emission is generally uniform around the torus.

Effects of impurity production on tokamak efficiency

The impurities have profound effects, some deleterious and some beneficial.

One of the most important effects of impurities is their contribution to the energy balance through their radiation losses, particularly due to heavy impurities. Because they are incompletely stripped over the entire plasma and radiate strongly. As the impurity increases, there is a point at which all the input power will be radiated away. The ultimate limits for the concentration of several elements under reactor like conditions (for D-T 50/50 plasma with total density 10^{14} cm⁻³ and $T_e = T_i = 10$ KeV) are shown in figure (2) [3]. For each element a fairly narrow range of concentration evidently exists for which its effect ranges from negligible to prohibitive for purpose of achieving energy break-even conditions. On the other hand, the radiative roll of light impurities is significantly different, like hydrogen light impurities are ionised and radiate predominantly at the plasma periphery (although, per atom, they radiate much more strongly than hydrogen) This is not necessarily a deleterious effect, because low Zn ion radiation at plasma edge helps in transferring the plasma energy rather harmlessly to the wall. Moreover, they also cool the edge and force the current density and hence the temperature and power input distribution to become more centrally peaked.

However, in the central hot region, where the confinement characteristics are really determined, these atoms are fully stripped and emit, not very strongly, only bremsstrahlung radiation.

Impurities also affect the plasma by determining the effective charge.

$$Z_{\text{eff}} = \sum \frac{N_z Z^2}{N_e} \tag{1}$$

Where sum is over all the existing ions of charge Z and density N_z . Z_{eff} enters into the formula for the plasma resistivity, i.e. it plays a role in shaping the plasma current and consequently, the input ohmic distribution. In this contest, low Z_N impurities are worst offenders, because the lower density of high Z_N impurity does not usually affect significantly the plasma resistivity. Generally, as the impurity content increases, confinement and stability decreases and instabilities develop progressively at lower N_e and I_p values. Other effects of impurities are changes in collisional transport coefficients across the confining magnetic field, reduction of the ratio N_i / N_e (N_i being the proton or deuteron density), which therefore reduces the neutron yield of deuterium plasmas at a given electron density, and reduction of the penetration of neutral beams (used for additional heating) due to large cross sections for electron capture by highly stripped impurities for hydrogen isotopes.

Light impurities are not necessarily bad for the plasma, because they help to evacuate the heat to the walls and keep down the peripheral temperature. However, when attempting to increase

Ne to its maximum possible value, light impurity radiation increases eventually leading to a major plasma disruption [4-6]. The effect of heavy impurities, such as iron, nickel, etc (metals characteristic of the wall and limiter) is significantly different from that of light impurities. A major difference is that unlike light impurities, heavy elements are not fully stripped in the centre of the discharge and therefore can contribute significantly to the discharge power balance by line radiation. Heavy impurities also appear early in the discharge. Generally less ionized observed ions of Ti, Cr, Fe and Ni belong to the Na like and Mg like sequences.

The lowest ionization potential of these ions is approximately 300 eV. If proper care is not taken in keeping heavy impurity concentrations low, the central power balance can be dominated by heavy impurity. Line radiation, eventually leading to hollow Te profiles [7], moreover, even a small amount of heavy impurities can prevent tokamak ignition by too large line radiation losses (figure 2).

As already mentioned, heavy impurity ions emit at short wavelengths (extreme VUV and X-rays spectral regions); however, they also have the peculiarity of emitting forbidden lines. These transitions, occurring between levels of the same parity, mainly pertain to ground state configuration (the only state strongly populated at tokamak plasma conditions) and originate from magnetic-dipole or electric quadrupole interactions. The photon emissivity of these lines is not negligible compared to that of allowed (electric-dipole) resonance lines in spite of their low radiative transition probabilities. The main interest of such forbidden lines in tokamak plasmas lies in their diagnostic applications. Fairly strong spectral lines of relatively long wavelength (above 1200 Å) arising from the high electron temperature region of the plasma, their long wavelengths allow the use of sophisticated 'visible' optical techniques (involving mirrors, lenses and windows), not feasible at shorter wavelengths. Forbidden lines of Fe, Cr and Ti have thus been used in tokamaks for ion density measurements [8], local ion temperature evaluations from their Doppler broadening [9] and plasma rotation from their Doppler shift

[10]. Forbidden lines at shorter wavelength have also been observed [11, 12], but they are, of course, less useful for diagnostic purposes.

Present work

In present work we have studied the radial profile of electron temperature and radial profiles of spectral emission from the plasma from knowledge of electron temperature and the electron/ion densities.

In studying the radial profiles of the spectral emission from the plasma, the variation of temperature across the plasma cross section plays vital role. Therefore an appropriate temperature profile has to be considered.

Fractional abundance of impurity ions in the plasma is mainly determined by the electron temperature. As we know that the temperature at the torus axis is maximum and it goes on decreasing towards the wall. Thus, the suitable radial profile which would fulfill the above said boundary conditions must be assumed.

The profile of electron temperature across the plasma can be considered to be of two types which are given by following equations.

$$T(R) = T_0[1-(R/R_0)^2] \tag{2}$$

$$T(R) = T_0[1-(R/R_0)]^2 \tag{3}$$

Where T_0 is axial temperature.

R is radial distance at a point in the torus.

R_0 is radius of cross section of plasma column. These two radial profiles are shown in figure (3). In the first profile (dotted curve) the temperature decline is slow as one goes from axis to the walls. The second profile (solid curve) shows fast decline of temperature as one goes from axis towards the walls. Usually first profile is considered suitable because it shows similarity with the Maxwellian distribution function. This nature of profile is in close agreement with the nature of graph plotted by TFR group [13].

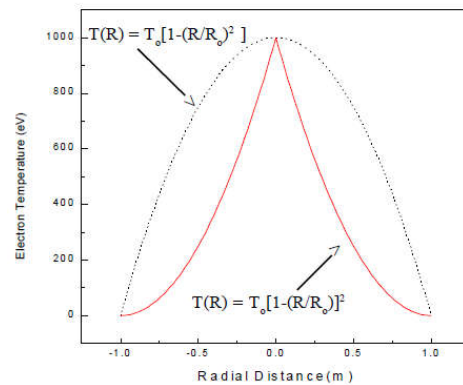


Figure 3:Radial Profile Of Electron Temperature(Te) In Tokamak Plasma For Te = 1000 eV.

RESULTS AND DISCUSSION

We have studied and obtained the radial profiles of fractional abundance of Fe I through Fe XXV at different axial electron temperature from 10 eV through 7000 eV. The radial profile of electron temperature is assumed to be like zero order.

Bessel function. Similarly, the radial profile of electron density is also assumed to behave like zero order function. The analysis of radial profiles of the ions show similar behaviour. We select profiles of few ions as typical cases and the results are presented below.

The radial profiles of Fe XXV in the plasma have been obtained for different axial electron temperature from 2000 eV through 7000 eV and the results are displayed in figure (4). The spatial distribution of Fe XXV ions show different behaviour at different electron temperatures. The shape of the profile at the electron temperatures on the axis of torus less than the electron temperature T_p at which the fractional abundance of Fe XXV ions is maximum is entirely different than the shape of profile at the electron temperatures on the axis of torus greater than the electron temperature T_p at which the fractional ion abundance is maximum.

It is clear that the curves are symmetric about the tube axis because it has been assumed that the tokamak plasma has axial

symmetry. At low axial electron temperature (say $T_0 = 2000$ eV), the fractional density of Fe XXV ions is maximum on the axis and minimum at the walls. As the axial electron temperature is increased the peak becomes flatter and rate of decrease of fractional abundance decreases as we go towards the wall from the axis. As the axial temperature is increased further (say $T_0 = 4000$ eV), the shape of curve changes from convex to concave showing a dip at the axis. If the axial electron temperature is increased further the dip becomes prominent with two side-peaks. And if the electron temperature is increased still further, the side peaks becomes sharper and they show their shift towards the walls of the tokamak. Similar profiles for few ions such as Fe XI and Fe XVI have been obtained and the results are shown in figure (5a), figure (5b), figure (6a), and figure (6b) respectively. The profiles show similar behaviour as those for Fe XXV ion. The behaviour of fractional abundance may be very well understood from the study of three dimensional plots of fractional abundance.

Typical three dimensional plots of the spatial distribution of Fe XVI ions for axial electron temperatures 225 eV, 300 eV and 400 eV are shown in figure (7), figure (8) and figure (9) respectively. The figures give very well feeling about the spatial distribution of fractional abundances of the ionic species.

It is observed that the fractional abundance shows a well shaped structure. If electron temperature is greater than the electron temperature corresponding to maximum fractional abundance T_p , the plot of the fractional abundance shows a hill shaped structure where as if the temperature on the axis is less than T_p , the fractional abundance show hill shaped structure. As the electron temperature on the axis is increased, the rim of the well goes on shifting towards the wall and the depth of the well goes on increasing.

Another three dimensional view of same ion with axial electron temperature 600 eV is shown in figure (10). From these plots of fractional abundance, it is observed that the region of maximum fractional abundance shifts towards the wall. Thus, we may say that if the axial electron temperature exceeds the electron temperature T_p corresponding to the maximum fractional abundance of the ion, and if it increases to higher values, the region of maximum fractional abundance of that ion shifts towards walls of the tokamak compared to that having axial electron temperature 400 eV in figure (9).

For getting better feeling about the spatial distribution of fractional densities, the three dimensional views of iron ions Fe XV for axial electron temperature 225 eV, 300 eV, 400 eV, and 600 eV are shown in figure (11), figure (12), figure (13) and figure (14) respectively.

The radial profiles of ions are very useful for knowing the fractional abundances of an impurity ion at a particular radial distance from the axis of the plasma column. The three dimensional presentation of impurity ions at particular axial electron temperature indicates spatial distribution of ions of interest. For example in figure (9), if the axial electron temperature is 400 eV, the Fe XVI ion have maximum fractional abundance at a distance 0.65 m from the axis and from the radial profile of electron temperature, we can determine the temperature at the point whose distance is 0.65m from the axis which is 231 eV. Thus the study of radial profiles

of the spectral emission and fractional ion abundance combinely, act as a powerful diagnostic tool in tokamak.

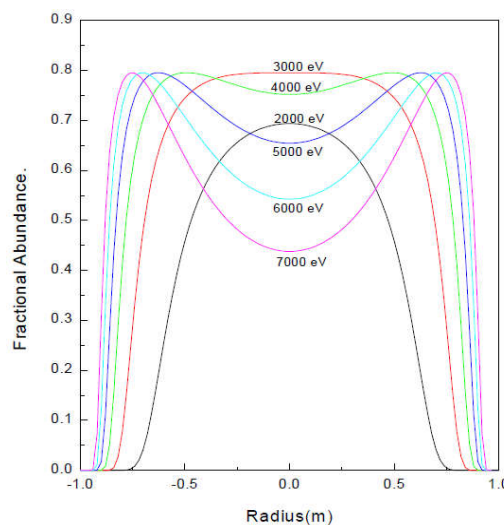


Figure 4 The Radial Profiles Of Fractional Abundance Of Fe XXV For Different Electron Temperatures On Axis Of TOKAMAK.

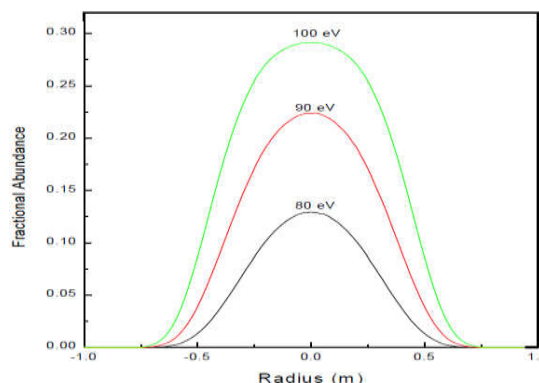


Figure 5 (a) : The Radial Profiles Of Fractional Abundance Of Fe XI For Different Electron Temperature ON The Axis Of The Tokmark.

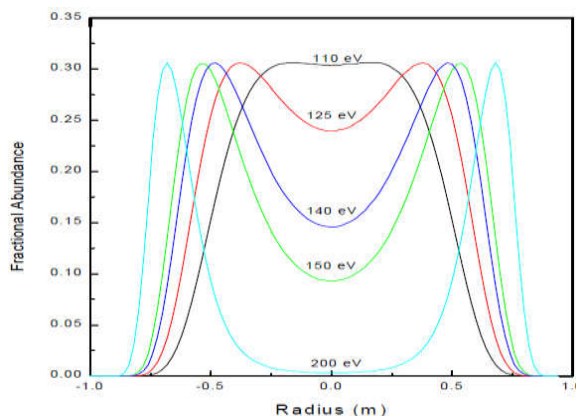


Figure 5(b) The Radial Profiles Of Fractional Abundance Of Fe XI For Different Electron Temperatures On The Axis Of The Tokamak.

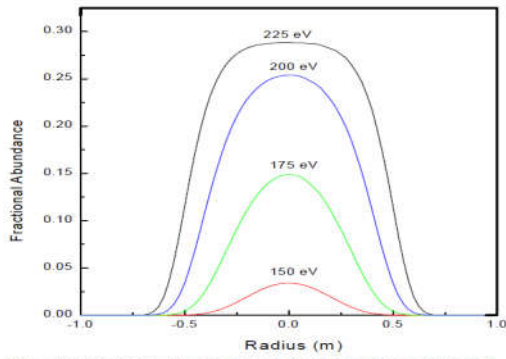


Fig. 6 (a) : The Radial Profiles Of Fractional Abundance Of Fe XVI For Different Electron Temperature ON Axis of Tokamak.

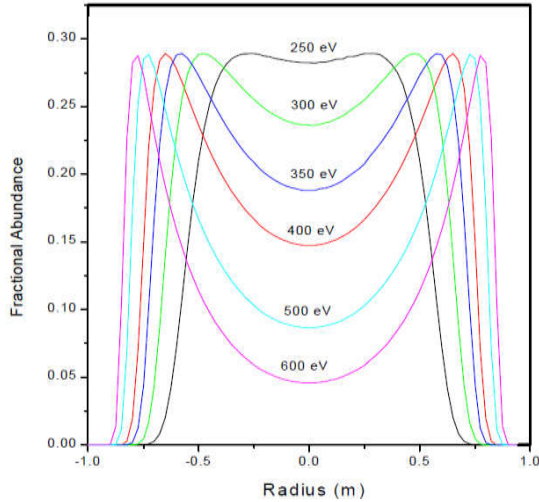


Fig 6 (b) : The Radial Profiles Of Fractional Abundance Of Fe XVI For Different Electron Temperatures On Axis of Tokamak.

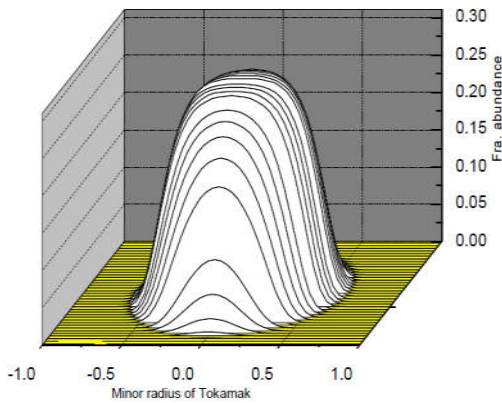


Figure 7 : Three Dimensional View Of Radial Profile Of Fe XVI When Electron Temperature At The Axis of Tokamak Is 225 eV.

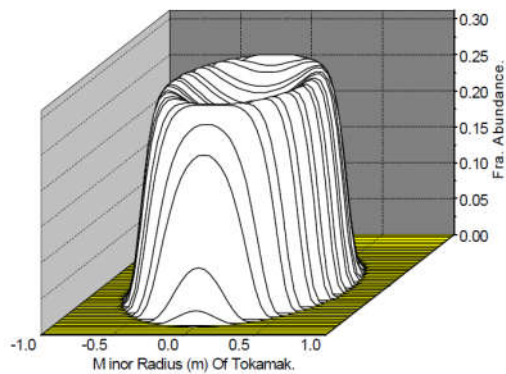


Figure 8 : Three Dimensional View Of Radial Profile Of Fe XVI When Electron Temperature AT The Axis Of Tokamak Is 300 eV.

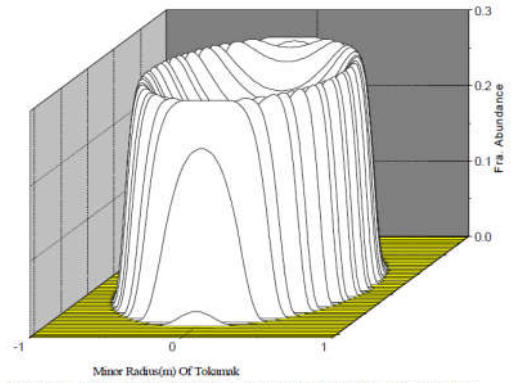


Figure 9 : Three Dimensional View Of Radial Of Fe XXVI With Electron Temperature At The Axis Of Tokamak Is 400 eV.

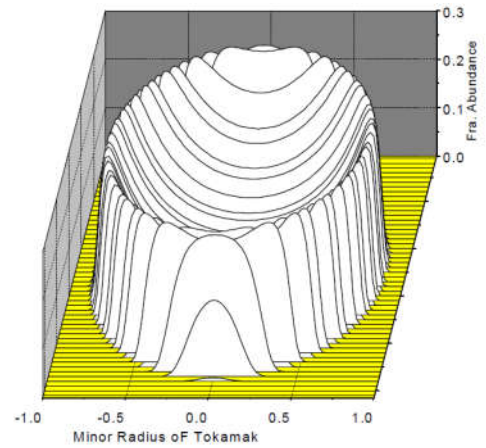


Figure 10 : Three Dimensional View Of Radial Profile Of Fe XVI When Electron Temperature At The Axis Of Tokamak Is 600 eV.

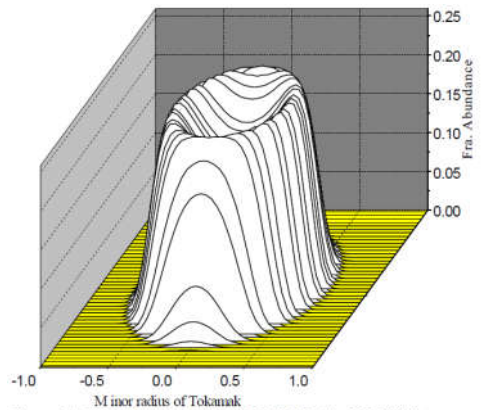


Figure 11 : Three Dimensional View Of Radial Profile Of Fe XV When Electron Temperature At The Axis Of Tokamak Is 225 eV.

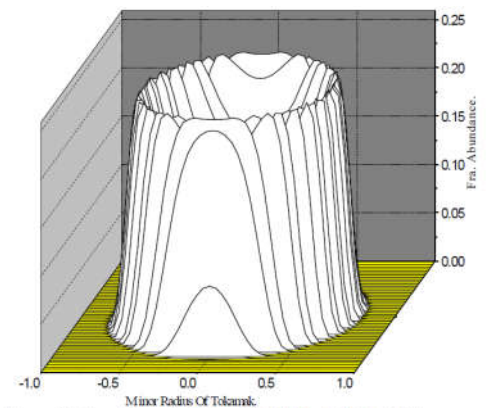


Figure 12 : Three Dimensional View Of Radial Profile Of Fe XV When Electron Temperature At The Axis Of Tokamak Is 300 eV.

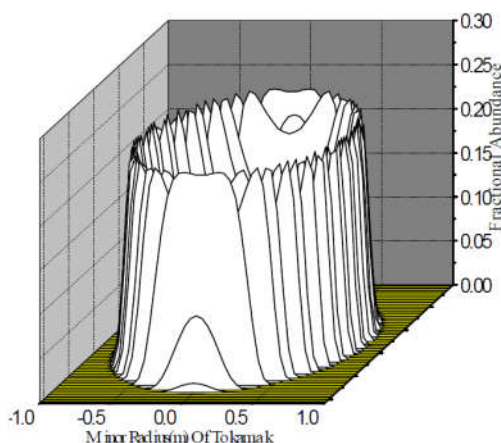


Figure 13: Radial Profile Of Fractional Abundance For Fe XV At 400 eV Electron Temperature.

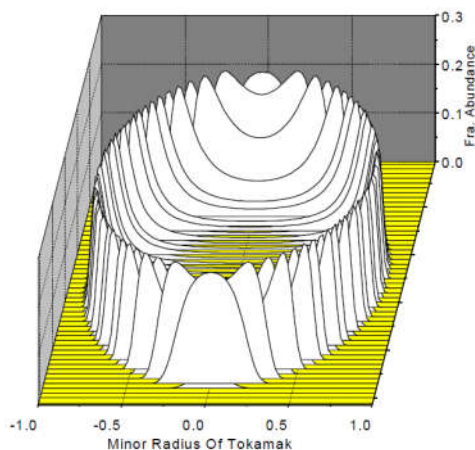


Figure 14 : Three Dimensional View Of Radial Profile Of Fe XV When Electron Temperature At The Axis Of Tokamak Is 600 eV.

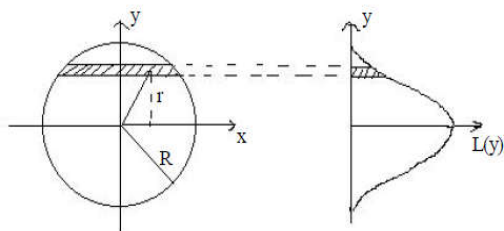


Fig:15 Observation of Cylindrically symmetric plasma.

Experimental arrangement for measurement of spectral radiance $L(\lambda)$ of the Tokamak plasma

The spectral radiance $L(\lambda)$ of the plasma which is measured in the unit watt per square meter per nanometer wavelength interval and per steradian. The local emission in the plasma is characterized by the spectral emission coefficient $\epsilon(\lambda)$ with the unit watt per cubic meter per nanometer wavelength interval and per steradian. The spectral radiance of optically thin plasma is obtained by integrating along the line of sight (x).

$$L(\lambda) = \int_a^b \epsilon(\lambda, x) dx$$

In the special case of cylindrical symmetry $\epsilon = \epsilon(r)$ local emission coefficients may also be obtained for inhomogeneous but optically thin plasma. Figure (15) illustrates the principle. The plasma is viewed perpendicular to the cylindrical axis, and the spectral radiance is recorded spectrally and resolved along the y-axis.

$$L(\lambda) = 2 \int_y^R \frac{\epsilon(r)}{(r^2 - y^2)^{1/2}} dr$$

This equation is of the Abel-type and can be inverted to obtain $\epsilon(r)$, the transformation being called Abel inversion [14,15]

References

De Michelis, C. and Aattioli, M., Rep. Prog. Phys. 47, 1233-1346(1984)
 Mc Crackan, G. M. and Stott, P. E., (1979), Nucl. Fusion, 19, 889-981.
 Jensen, R. V., Post, D. E., Grasberger, W. H., Tarter, C. B. and Lokke, W. A., (1977), Nucl. Fusion, 17, 1187-96.
 M eisel, D. *et al* (1977), Proc. 6th Int. Conf. On plasma Physics and controlled Nuclear Fusion Research, Berchtesgaden, 1976 Vol. 1 (Vienna: IAEA) pp 259-64.
 Equipe TFR (1977a), Nucl. Fusion, 17, 1283-96.
 Toi, K., Itoh, S., Kadota, K., Kawahata, K, Noda N., Sakurai, K., Sato, K., Tanqhashi, S. and Yasue, S. (1976). Nucl. Fusion, 19, 1643-63.
 Hawryluk, R. J. *et al* 1979b Nucl. Fusion 19, 1307-17.
 Suckewer, S. *et al* (1979b) Nucl. Fusion 19, 1681-1683.
 Suckewer, S. and Hinnov, E. 1978 Phys. Rev. Lett. 41, 756-9.
 Suckewer, S. Eubank, H.P., Goldston, R. J., Hinnov, E. and Sauthoff, N. R. (1979a) Phys. Rev. Lett. 43, 207-10.
 Klapisch, M., Barshalom, A., Schwob, J. L., Fraenkel, B. S., Breton, C. De Michelis, C., Finkenthal, M. and Mattioli, M. 1978a Phys. Lett. 69A, 34-6.
 Klapisch, M. Schwob, J. L., Finkenthal, M., Fraenkel, B. S., Egert, S., Barshalom, A., Breton, C., De Michelis, C. and Mattioli, M. 1978b Phys Rev. Lett. 41, 403-6.
 TFR group, Plasma Physics, Vol.19, pp-349 to 361 Pergamon press, 1977, printed in Northern Ireland.
 Griem, H. R., "Plasma spectroscopy ", McGraw-Hill, New York, 1964.
 Smeulders, P., Nucl. Fusion, 26, 267 (1987).

How to cite this article:

Jadhav A.N.2016, Impurity Production in Tokamak and Their Radial Profiles. *Int J Recent Sci Res.* 7(8), pp. 13021-13026.